

S55 PROJECT – CFD ANALYSIS OF AN HISTORICAL SEAPLANE

Baldon C.¹, Indelicato R.¹, Bottino N.¹, Sinisi M.¹, Carrone F.¹, Cantanna G.¹, Cestino E.¹, & Sapienza V.²

¹ Politecnico di Torino, Turin, Italy

² Aeronautical Engineering Consultant, Turin, Italy

Abstract

The aerodynamic properties of the Savoia Marchetti S55-X model aircraft, in construction by the student team “Team S55”, are studied in order to evaluate its aerodynamic behavior in cruise flight configuration. The Computational Fluid Dynamics software Star CCM+ and ANSA have been used to simulate the model aircraft at various angles of attack, with the objective of studying the lift and drag coefficient changes at every angle. The analyses showed a good consistency with the data previously calculated using semi-empirical formulae and with the original experimental data obtained by testing the S55-X aircraft in the wind tunnel.

1. General Introduction

The aeronautical industry is getting bigger by the day, with new challenges continuously arising and requiring constant evolution both in terms of design and technologies. The tools that allow the analysis and construction of an aircraft have deeply changed during the last decades and the vast majority of these improvements were made thanks to the advent of the computer era: this is the context where Team S55, a student team from Politecnico di Torino, was born. The main goal of the team is to apply state of the art methodologies to the aircraft design of a very important historical seaplane, the Savoia Marchetti S55-X. The short-term objective is to build a flying 1:8 scale replica of this famous Italian aircraft, while has as a long-term goal to be capable of building a full-scale replica using innovative materials and design technologies. For the past two years, the aerodynamics section of the team has been focusing on the study of the aerodynamic behaviour of the seaplane thanks to the use of Computational Fluid Dynamics (CFD) software. In this paper the methodologies applied for the analyses and a first set of results will be shown. First, the CFD features and models will be discussed. Then a description of the studies for the various configurations will be reported, followed by the respective results in terms of aerodynamic performances. More specifically, there are going to be three main types of analyses. The first one presented will be the simulation of the lifting elements of the seaplane’s scale model, the second one will be the analysis of the complete aircraft during the cruise flight phase and the third one will be a preliminary study of the take-off performance on water. This last analysis will be including the hydrodynamic drag modelling and preliminary considerations on the simulation of the aircraft in the take-off phase of the flight.

2. Methodologies For The Analyses With CFD Software

Two different software have been used by the team in order to correctly analyse the aerodynamic properties of the model aircraft. For the simulations on wings and tail the computational fluid dynamics software Star CCM+ has been used, while to analyse the whole aircraft, the decision of using Star CCM+ in combination with the ANSA software has been made. For this purpose, as shown in Table 1, the ANSA software has been used for the preparation of the different surfaces and for the meshing phase, while the physics conditions setting, the simulation phase and the post processing phase have been conducted in Star CCM+.

Table 1 - Software used for each step in the analyses

	Surface Preparation	Boundary conditions	Surface and volume meshing	Physics conditions	Simulation	Post Processing
ANSA	✓	✓	✓			
Star CCM+		✓		✓	✓	✓

2.1 CAD Geometries and Meshing

The CAD geometry has been imported into the environment of the ANSA software. Due to the need to obtain data in order to confirm the consistency of the assumptions that had been made for the preliminary design of the model aircraft, the geometry that has been used for these analyses does not present the tail booms and the engine mount structure. In order to obtain a suitable geometry for the CFD analysis, it has been simplified to an outer shell by removing all internal components to reduce its computational weight and then repaired through ANSA's geometry tools. This action prevented the generation of invalid mesh elements, usually found near the trailing edges of the lifting elements or around junction points of rudders and stabilizer. A valid and more accurate mesh helped obtaining more precise analyses and eased the convergence process of the simulations [8].

Using the ANSA meshing software, the nodal points for the discretization of the aircraft's surface were accurately placed, having paid

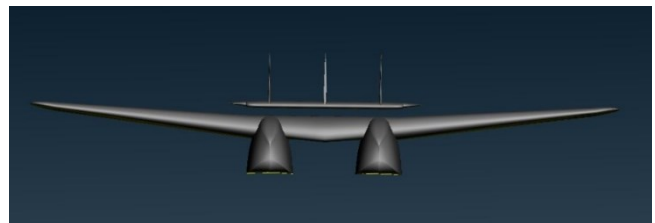


Figure 1 - Frontal view of the CAD geometry used

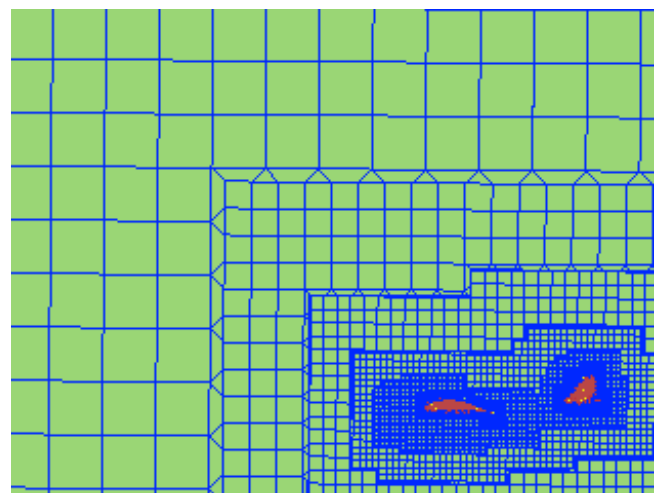


Figure 2 - View of the increase in mesh size

special attention to all those critical geometry parts which require a more refined discretization, such as leading edges and junction points. The surface mesh was then generated from those nodal points, becoming the basis from which the first mesh is extruded. This first volume mesh created a Prism Layer shell in order to better analyze the behavior of the boundary layer between the surface of the aircraft and the external flow. The thickness of the first cell, as well as the thickness progression of the Prism Layer mesh, was determined on the basis of the wall y^+ value to ensure that the first cell center from the wall is contained in the log-law region of the boundary layer [6].

Ultimately, the volume mesh was produced by extrusion, starting from the outer surface of the prism layer. This mesh can be divided into two main regions, each containing different types of cells. In the inner region, “tetra” elements, consisting in prisms with a triangular or rectangular base and pyramids, are found near the surface. For the outer and bigger region of the domain, an “hexa interior” mesh was generated: it consists of a standard cubic mesh with prisms and pyramids ensuring a clean transition between cubic elements of different sizes. This particular kind of mesh proved to be the most suitable for the simulation of external flows, since it generates less cells in the outer region of the computational domain than a tetrahedral mesh and is well capable of generating refinements in the flow separation zones. Moreover, the related computational cost was relatively low, making it a very good compromise between accuracy and cost [8].

2.2 Physics Models and Solvers

Most of the simulations tested the model aircraft in cruise trim, therefore the resultant of the forces and torques applied on it was zero and the plane was moving at a constant speed. In order to comply with this assumption, these simulations didn't allow any degree of freedom: any resulting torque or unbalanced force in the simulation had to be due to a different position of the moving surfaces of the model. Taking these forces and torques into account would require for much more complex and specific analyses to be done.

The Reynolds number of the system was calculated to be approximately $1.03 \cdot 10^6$, based on the measured chord of the wing's root and for a cruise speed of 21.7 m/s. This value meant that an important assumption could be made: the presence of periodical phenomena (e.g. the Von Karman wake, typical of lower Reynolds numbers), which would require a time unsteady simulation to be able to capture the behavior of the aerodynamic interactions and have a precise result, could be assumed to be negligible, therefore a time steady model has been used [7].

The main model used for all the simulations is the segregated flow model. The reason for this particular choice for the analyses lies in the fact that this solver, which is less burdensome than the coupled one, has proven to be the best choice in absence of high pressure fluctuations and at low Mach numbers, since the choice of these models had to be guided by the need to find the best compromise between computational cost and precision of analysis [7].

The external flow is considered as an ideal gas and the standard air conditions were maintained as constant, assuming the effects depending on altitude changes to be negligible. This assumption has been justified by the low altitude parameters of the cruise flight phase of the model aircraft.

The calculated Reynolds number also suggests the need for the analyses to include turbulence models, being it much superior than the indicative target figure for a transition between a laminar to a turbulent boundary layer.

Two-equation models for the turbulence of the external flow have been used for the simulations. The good performance of k-epsilon model, solving the equations for turbulent dissipation and kinetic energy, for the simulation of an external flow with a high Reynolds approach, together with the lower

computational cost led to the decision to choose it over the k-omega model, which instead solves the equations for kinetic energy and turbulent frequency and is more suitable for a low Y^+ approach, to analyze the performance of the complete aircraft model during the cruise flight. This decision has been made also taking the global physics into consideration, since the aircraft is not subjected to an extremely turbulent flow and there are no shocks, violent flow separations or combustion zones to analyze [7].

3. First Analyses on Lifting Elements

Before studying the full three-dimensional wing CAD geometry, a set of two-dimensional analyses on the wing airfoils has been carried out in order to obtain initial data in terms of pressure coefficient distributions on the upper and lower wings, as shown in Figure 3. The purpose of these first simple simulations has been the confirmation of the preliminary esteem of the aerodynamic forces on the aircraft model which had been carried out by the Flight Mechanics section of the team in its early days, first using a simplified model immersed in a non-viscous flow and then adding the contribution of the viscous interactions with the help of semi-empirical formulae. The meshes for these first analyses have been fully developed in STAR-CCM+.

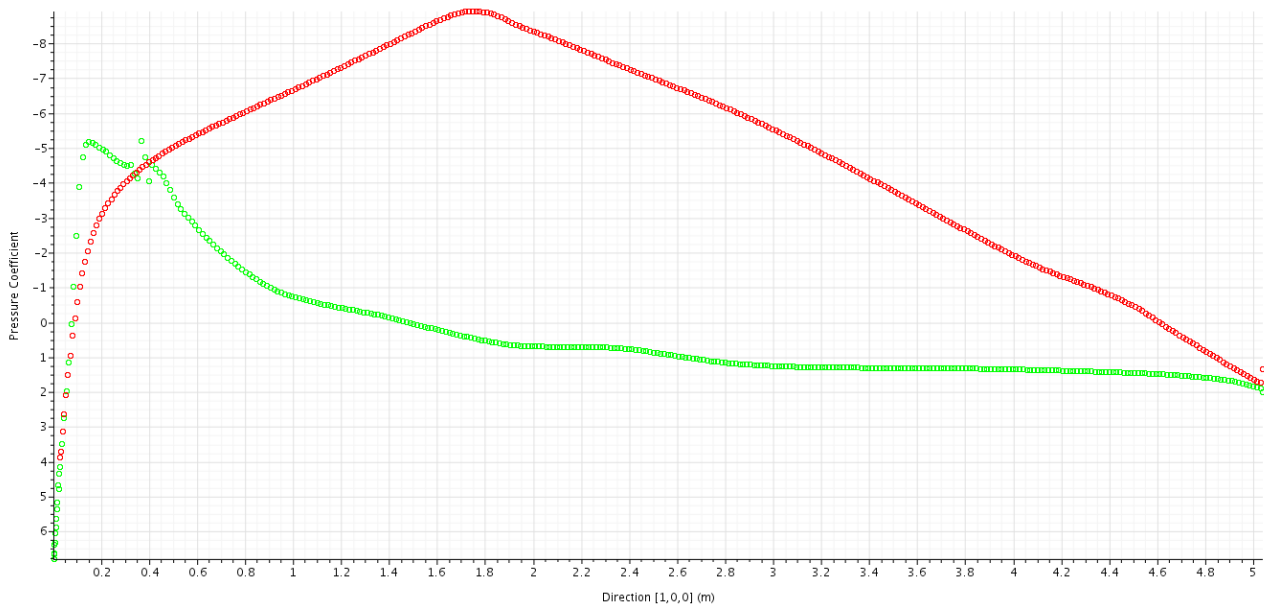


Figure 3 - Pressure coefficient distribution on the airfoil at the root of the wing

4. Cruise Analysis

This type of analyses have been conducted for the cruise phase of the flight, thanks to the combination of the two different software:

- ANSA for the pre-meshing and the definition of the mesh levels;
- Star-CCM+ for the choice of both physics models and boundary conditions, as well as the simulation process and post-processing.

The main goal of the preparation of this simulation is the creation of a geometry model free from

imperfections and as light as possible concerning the computational cost of the analysis, but also the generation of the various layers of the mesh, for the creation of which the minimum imperfection in the geometry, such as gaps or poorly rendered surfaces would cause the entire process to fail [8].

Once the geometry of the aircraft has been rendered suitable for the discretization, a mesh sensitivity study has been set up in order to find the best compromise between mesh quality and number of mesh cells.

The last action required for the simulation set up is the physics models choice, here focused on the cruise settings.

4.1 Geometry and Meshing

For this process the software ANSA from Beta CAE Systems has been used. The work has started with a preliminary cleaning of the surfaces, i.e. the deletion of some internal elements such as stringers, ribs and longerons, to prevent the creation of useless mesh elements. Then, appropriate bonds between external surfaces have been created in order to set up a clean assembly where to generate the surface mesh. Ultimately, the last step of this preliminary phase has been improving the aspect of complex geometries, such as the wing tips couplings. The resulting geometry is shown in Figure 4.

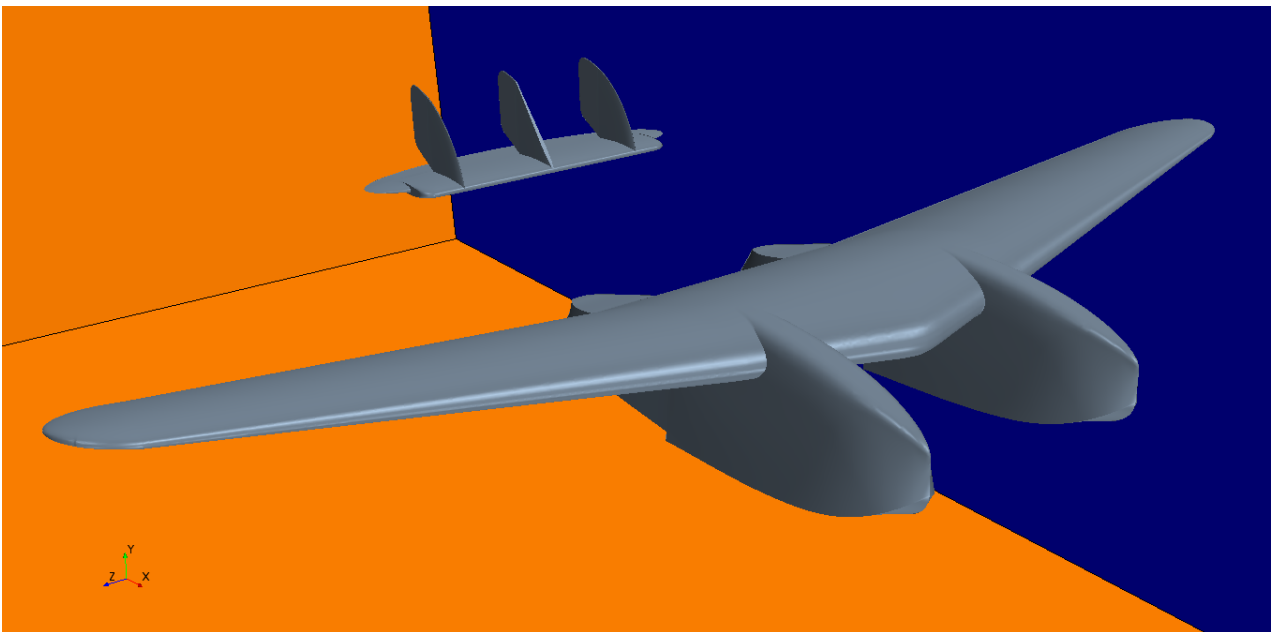


Figure 4 - CAD geometry after the cleanup

Once the CAD preparation has been completed, the different mesh levels have been generated.

- Surface mesh: an accurate discretization with a specific refinement on those elements which are more subject to critical changes in pressure due to airflow impact, as well as on areas featuring major curvatures. Figures 5 and 7 show details of the surface mesh described and the parameters here used are reported in table 2.

Table 2 - Surface mesh parameters

	Minimum surface size (mm)	Maximum surface size (mm)
Model	5	30
Domain	30	300

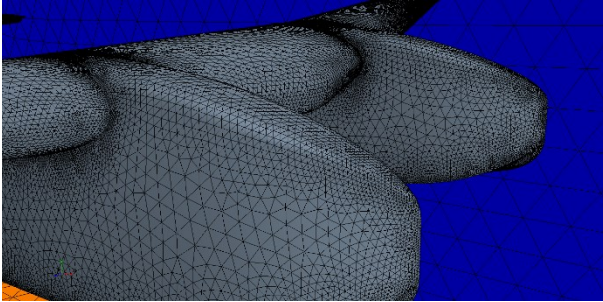


Figure 6 - Surface mesh on the hulls of the model

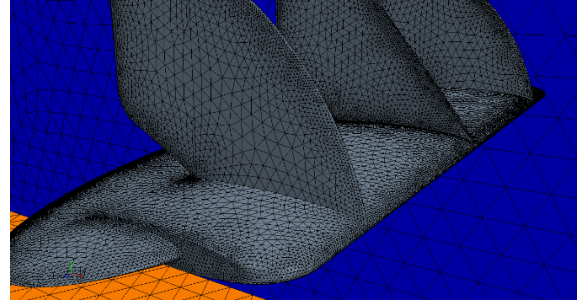


Figure 5 - Surface mesh on the tail of the model

- Prism layer mesh: nine layers with increasing thickness as a function of the wall distance, in order to best simulate the behaviour of the boundary layer.
- Volume mesh: featuring two different types of elements, tria (pyramidal or triangular based prismatic elements) and hexa (cubic elements), starting from a very fine cover around the aircraft and growing into a coarser mesh at the far field. The generated volume mesh is shown in Figure 7.

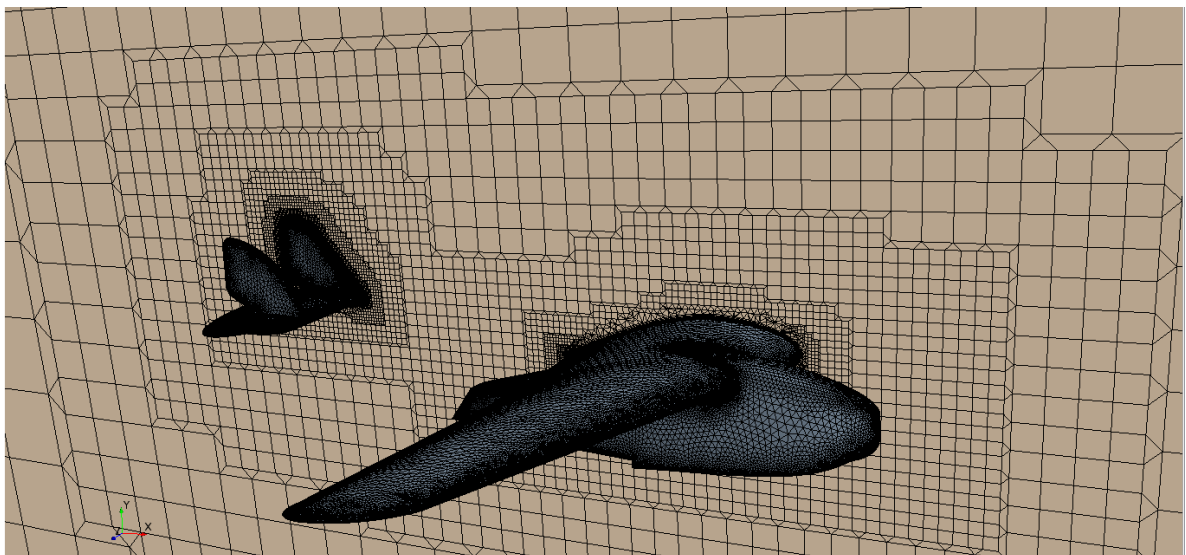


Figure 7 - Volume mesh on the computational domain near the model

4.2 Simulation and Results

After the output of the volume mesh from ANSA to the Star CCM+ software, the definition of the correct physics of the domain and the preparation of the reports, a set of simulations has been conducted on the aircraft at various angles of attack, in a range going from -10 to +18 degrees, including one at an angle of -5.37 degrees which is the attack angle for the cruise flight configuration. The resulting values for the lift and drag coefficients are reported in Table 3. Figures 8 and 9 show respectively the pressure field and the velocity field around the surfaces of the model aircraft. It has then been possible to interpolate the collected data, in order to visualize the drag coefficient and lift coefficient trend with the angle of attack, as shown in Figures 11 and 12. It is possible, at this point, to notice that the lift coefficient trend shows the aircraft reaching the stall at +16 degrees. However, this particular datum does not take into consideration the presence of the propeller on top of the cabin of the aircraft which would cause an increase of the drag and would change the behavior of the flow over the central plane of the model causing it to stall before reaching such an angle, so it has been only considered as a first estimate of the stall angle and will be corrected after calculating it with a CFD analysis on a more precise assembly in terms of geometry and elements.

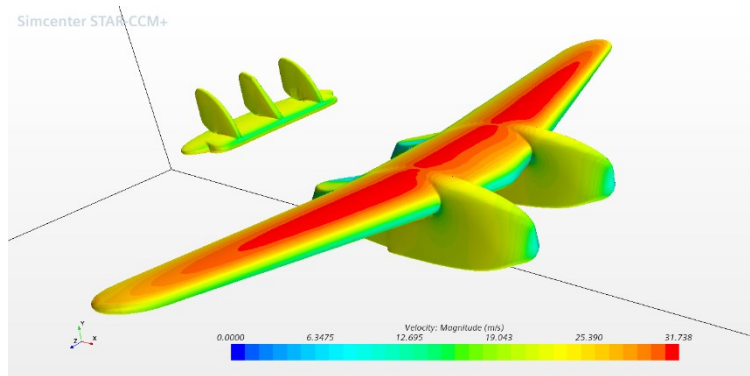


Figure 8 - Velocity field around the aircraft

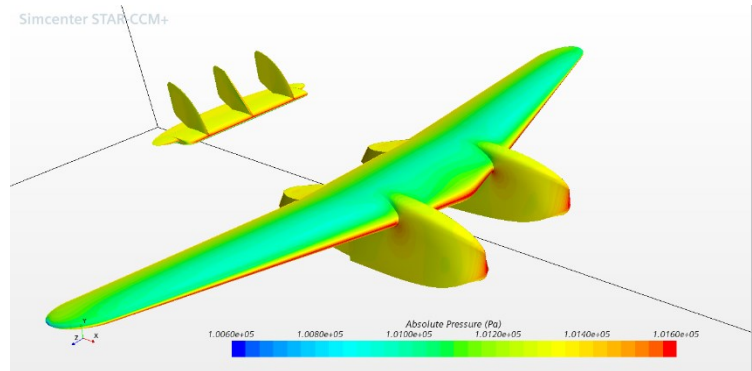


Figure 9 - Pressure field around the aircraft

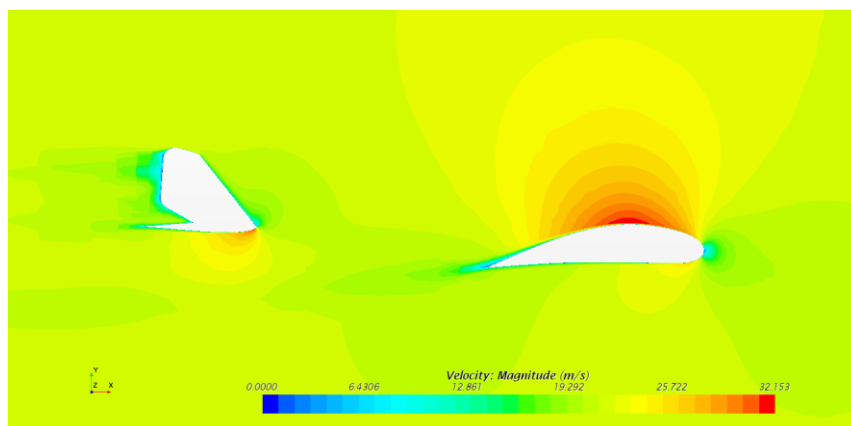


Figure 10 - Velocity field over a wing and a rudder

Table 3 - Collected data for lift and drag coefficients

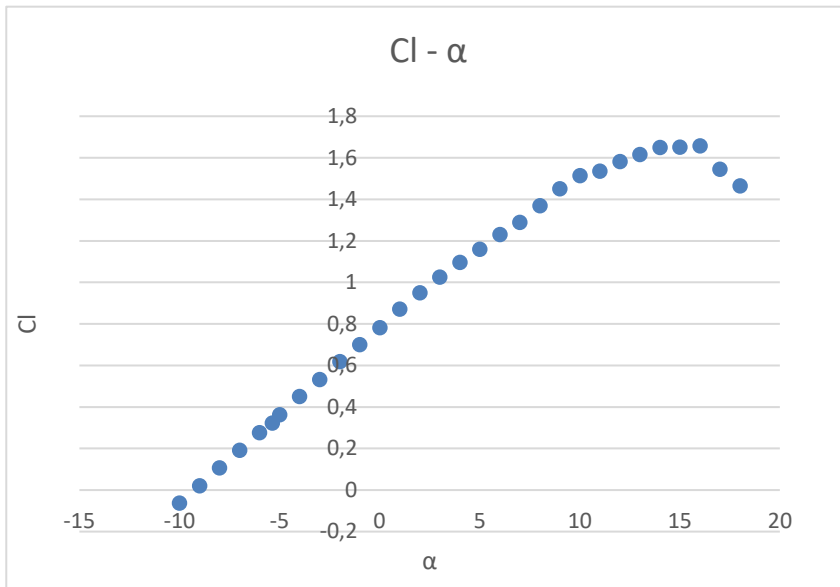


Figure 11 - Lift Coefficient trend

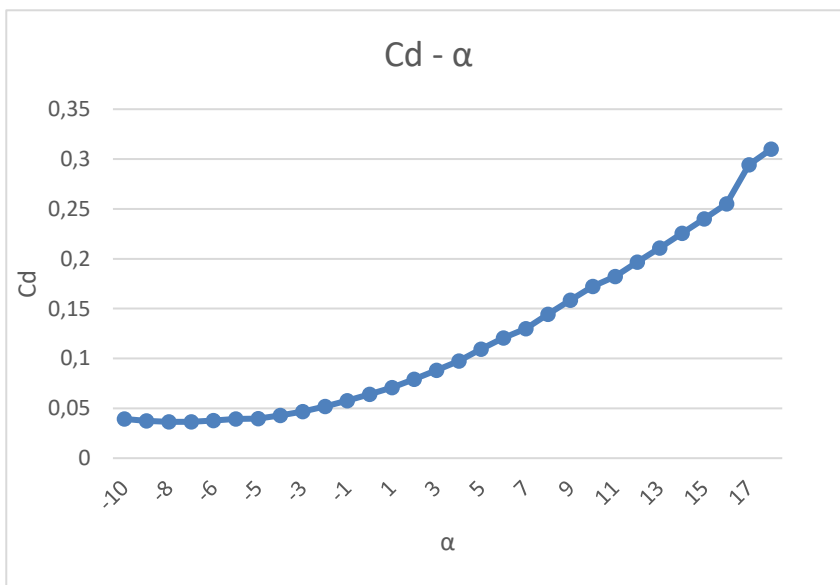


Figure 12 - Drag Coefficient trend

α	Cl	Cd
-10	-0,0632	0,03927
-9	0,02	0,03752
-8	0,1059	0,03642
-7	0,1914	0,03646
-6	0,2765	0,03759
-5,37	0,323	0,0392
-5	0,3624	0,03974
-4	0,4503	0,0429
-3	0,5318	0,0468
-2	0,6183	0,0519
-1	0,7001	0,0577
0	0,7823	0,0642
1	0,871	0,0708
2	0,949	0,0792
3	1,0245	0,0882
4	1,0962	0,0976
5	1,1601	0,1094
6	1,2304	0,1207
7	1,2887	0,1298
8	1,3688	0,1444
9	1,4508	0,1583
10	1,5139	0,1724
11	1,5352	0,1823
12	1,5819	0,1968
13	1,6155	0,2108
14	1,6497	0,2255
15	1,6513	0,2401
16	1,6566	0,2551
17	1,5451	0,2943
18	1,465	0,3099

With the collected data, an important comparison could be also made. The drag and lift coefficient values have been interpolated in a drag polar curve, which was put in comparison with the one previously obtained. This second curve had been computed using the Athena Vortex Lattice (AVL) calculation software, which simulated the aircraft in a non-viscous flow [9], and then a viscous contribution had been added using semi-empirical formulae. The comparison between the two polar

curves, as shown in Figure 13, highlights the correctness of the collected data, as well as the superior precision of the CFD simulation in obtaining such values, which is the reason of the difference between the two curves.

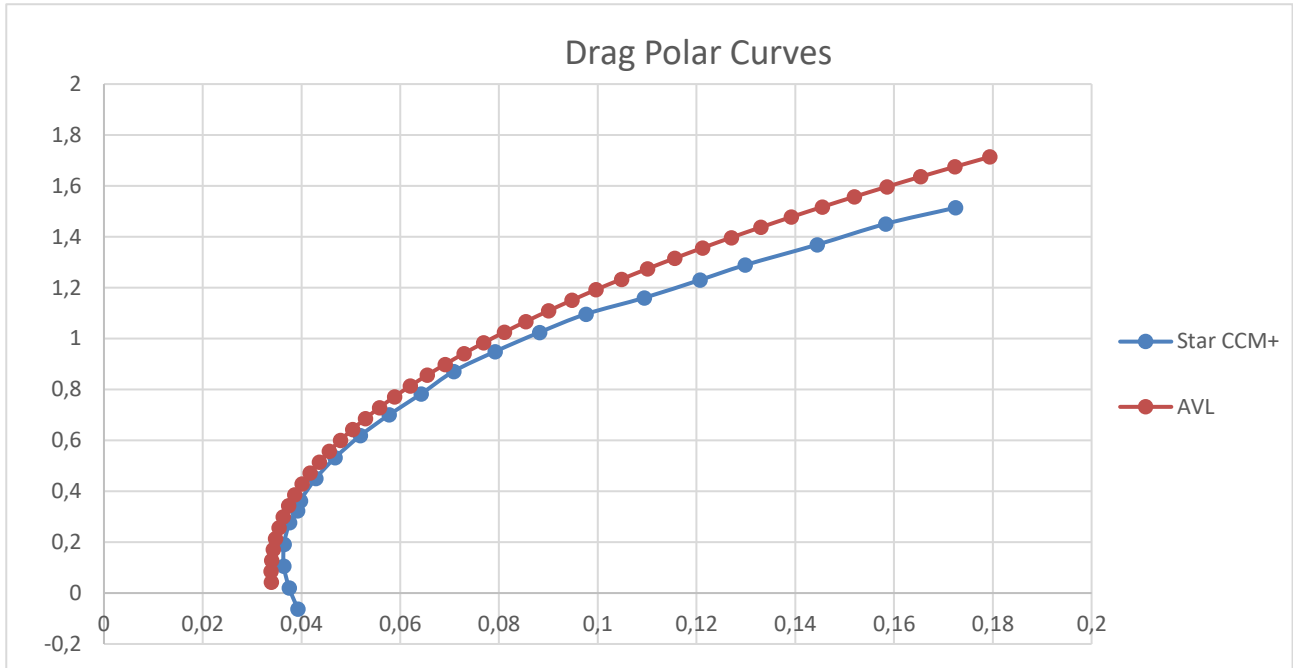


Figure 13 - Comparison between the two drag polar curves

The calculated data for the lift and drag coefficients were also ultimately put in comparison with a set of experimental data, which had been obtained for the original SIAI Marchetti S55-X [4] in the wind tunnel. From the confrontation of these curves, shown in figure 14, it is possible to notice the good correspondence at low angles of attack, and the fact that for higher angles the lift coefficient is lower than the one obtained in the simulations. This difference is due to the simplified geometries used for the calculations on the model airplane, as well as the fact that the Reynolds number of the flow on the model aircraft is different from the one affecting the original aircraft, thus not ensuring the similitude between the two airflows.

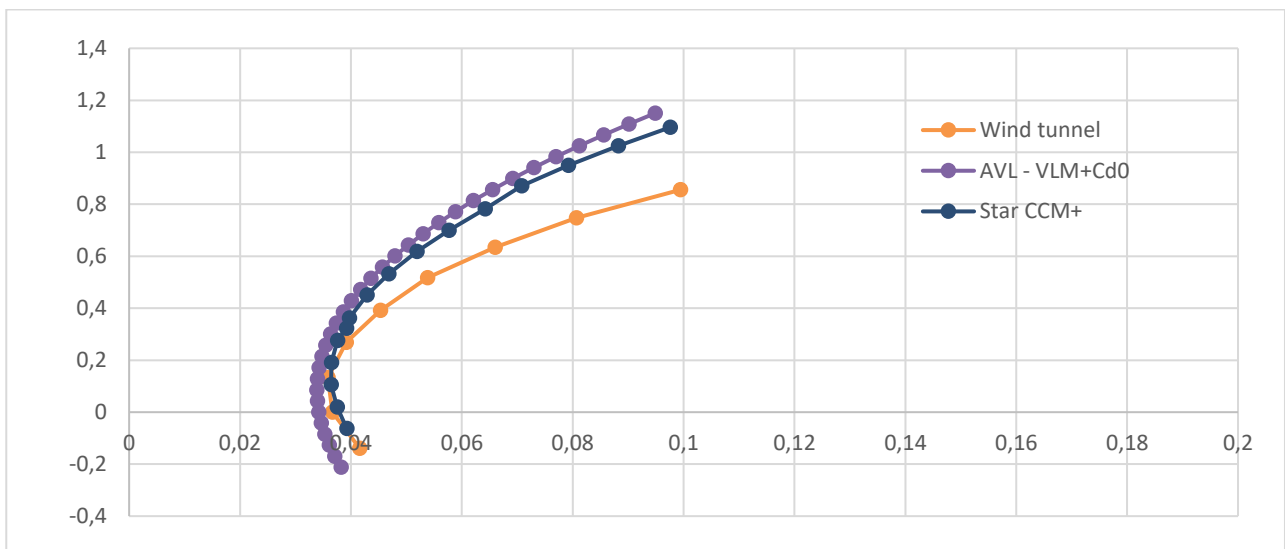


Figure 14 - Comparison between analytic and historical experimental data

5. Take-off Performance

The first step of this analysis involved the calculation of an estimate of the model aircraft's take-off distance. In order to do so, a study of the aircraft's behaviour during its take-off run in calm water was conducted. The model aircraft's hump speed was calculated with the following equation:

$$V_h = T_q \sqrt{L} \quad \text{Eq. 1}$$

Where V_h is the hump speed expressed in knots, T_q is a coefficient which has a value of 3 for planing hulls, and L is a characteristic length expressed in feet. The resulting hump speed was 3.05 m/s, approximately 15% of the speed required for the model aircraft to take off. At this speed, the value of the hydrodynamic resistance reaches its peak of about 20% of the total weight of the aircraft and starts decreasing as the hulls emerge from the water surface and start planing on it. Due to the complexity of calculating the exact hydrodynamic resistance during the run, it was then assimilated to a rolling friction approximately of 15% of the difference between the weight and the generated lift of the aircraft model [2]. Although the examination of references [3], [4], and [5] showed that for well-designed seaplanes this resistance could be lesser than that, this value was chosen to maintain a high conservativeness of the calculation.

The estimated take-off length was then computed using the MATLAB software to solve the following integral:

$$l = \int_0^{V_{to}} \frac{\frac{W}{g} V}{-\frac{1}{2} \rho V^2 S C_d + f * \left(W - T \sin(\Omega) - \frac{1}{2} \rho V^2 S C_l \right) + T \cos(\Omega)} dV \quad \text{Eq. 2}$$

Where $f = -0.15$ is the coefficient modelling the hydrodynamic drag affecting the aircraft and Ω is the propeller pitch angle, set at 8.5 positive degrees from the body axis of the aircraft model. The thrust provided by the two electric motors driving the two counter-rotating propellers in take-off conditions has been calculated as 10 Kilogram-force during a series of traction tests on the propellers of the aircraft in the laboratories of the Department for Mechanics and Aerospace (DIMEAS) of Politecnico di Torino. The calculation returned the result for the estimated take-off distance of 49 metres.

5.1 Preliminary Considerations on the Simulation of the Take-off Phase

After this first estimate of the take-off maneuver distance, the aerodynamics section of the team has decided to move to the computational analysis of this critical phase of the flight. In order to study the performance of the model aircraft during the take-off manoeuvre, a scenario allowing two degrees of freedom (vertical movement and pitching rotation) had to be chosen to take account

of all the moments and disturbance forces developed by the movement of the aircraft in this flight phase.

As a first action, required to correctly simulate these forces and moments, the position of the centre of mass of the entire aircraft has been identified and the relative moments of inertia have been calculated.

This specific kind of analysis points out the need for the realization of two meshes. The first one, the overset mesh, shown in Figure 15, created a 'control volume' joined with the body of the model aircraft and moved with it according to its degrees of freedom. The second one was meant to discretize the whole computational domain. After having defined all the correct interfaces between the two meshes, the related degrees of freedom are set using the DFBI (Dynamic Fluid Body Interaction) tool, and the physics of the simulation has been set up as using the VOF (Volume of Fluid) option, which allows to define the position of the surface between two eulerian phases, being in this case air and water, and the relative velocities of the two fluids. Such an analysis requires also the use of an unsteady time step [7].

It is certain that simulating an aircraft with this configuration is extremely expensive and heavy from a computational point of view. On that account, it has been decided to simulate just a single hull of the aircraft, modifying its properties to match those of the entire plane in terms of weight, inertia and centre of mass, as shown in figure 5.1. The simulation is going to run on the University High Performance Computing Cluster, in order to minimize the required time for the analysis and to have the possibility to use a more precise mesh.

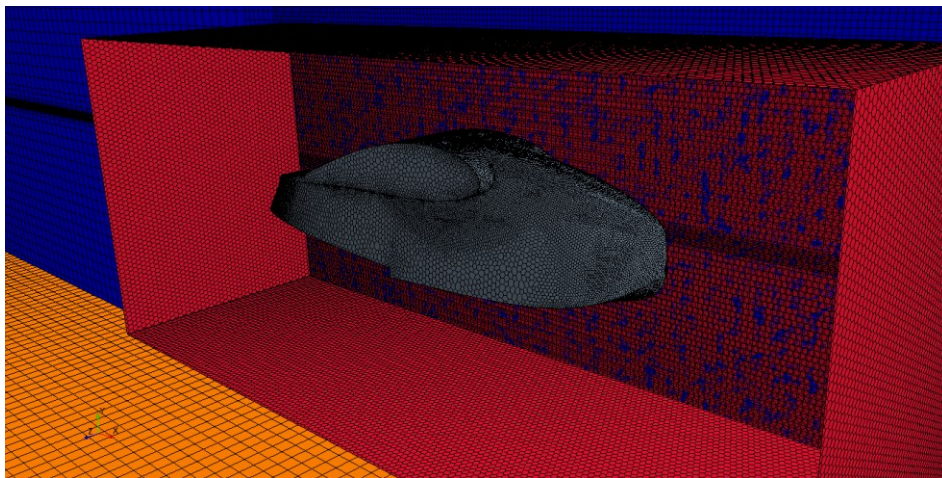


Figure 15 – Surface mesh and overset volume mesh on the hull

6 Conclusions

Thanks to the use of the CFD technology, a group of students has been able to analyze the aerodynamic behavior of the S55 seaplane and derive some useful data for the future construction of a Replica of this historical aircraft. Starting from simple simulations of the wing and the tail, the team has become skilled enough to run the analysis of the entire model aircraft so to explore its strengths and weakness during the flight. Furthermore, a study of the take-off performance has been conducted, giving results for the required take off length of the model aircraft. Concerning this topic, a CFD simulation has been set up, in terms of physics and mesh parameters. Given the nature of this study, the leap in complexity from the previous studies is huge. Further work will involve this kind of analyses and the matching semi-empirical results in possession of the team will be verified.

7 Contact Author Email Address

Mail to: enrico.cestino@polito.it

8 Copyright Statement

The authors confirm that they, and/or their company or organization, hold copyright on all of the original material included in this paper. The authors also confirm that they have obtained permission, from the copyright holder of any third party material included in this paper, to publish it as part of their paper.

The authors confirm that they give permission, or have obtained permission from the copyright holder of this paper, for the publication and distribution of this paper as part of the ICAS proceedings or as individual off-prints from the proceedings.

References

- [1] Cestino E., Sapienza V., Frulla G., Pinto P., Rizzi F., Zaramella F., Banfi D. *Replica 55 Project: A wood seaplane in the era of composite materials*, Politecnico di Torino, Sep 2018.
- [2] Chicken S.H. *Conceptual design methodologies for waterborne and amphibious aircraft*, PhD in Aerospace Vehicle Design, Cranfield University, 1999.
- [3] Truscott S. *The wave suppressors used in the NACA tank*, NACA TN-513, Dec 1934.
- [4] Truscott S., Parkinson J.B., Ebert J.W., Floyd Valentine E. *Hydrodynamic and aerodynamic tests of models of flying boat hulls designed for low aerodynamic drag*, NACA TN-668, Oct 1938.
- [5] Parkinson J.B. *The design of the optimum hull for a large long-range flying boat*, NACA ARR L4I12, Sep 1944.
- [6] Salim S.M., Cheah S.C. *Wall y^+ Strategy for dealing with wall bounded turbulent flows*, International MultiConference of Engineers and Computer Scientists, Jan 2009.
- [7] *Star CCM+ 2020.1 Documentation file*, Siemens Manual, 2020.
- [8] *Ansa for CFD Brief User Guide*, BETA CAE Systems, 2020.
- [9] Drela M., Youngren H., *AVL 3.36 User Primer*, retrieved from https://web.mit.edu/drela/Public/web/avl/avl_doc.txt, 2017.